Chemistry

Physical & Theoretical Chemistry fields

Okayama University *Year* 1987

Photoluminescence spectra and vibrational structures of the srs:ce^{3+} and srse:ce^{3+} phosphors

N Yamashita
Okayama University

Y Michitsuji
Okayama University

S Asano
Okayama University of Science

Photoluminescence Spectra and Vibrational Structures of the SrS:Ce^{3+} and SrSe:Ce^{3+} Phosphors

N. Yamashita and Y. Michitsuji[1]

Department of Physics, Faculty of Science, Okayama University, Tsushima, Okayama 700, Japan

S. Asano

Department of Electronic Engineering, Faculty of Technology, Okayama University of Science, Ridai-cho, Okayama 700 Japan

ABSTRACT

The details of photoluminescence and excitation spectra of powder phosphors were obtained at various temperatures between 6 and 300 K. At 300 K, two emission bands originating from the $^2T_{2g}(5d) \rightarrow {}^2F_{7/2}, {}^2F_{5/2}(4f)$ transitions are observed at 480 and 535 nm for SrS:Ce^{3+} and at 470 and 527 nm for SrSe:Ce^{3+}, respectively. In the excitation spectra, bands corresponding to the $^2F_{5/2}(4f) \rightarrow {}^2T_{2g}(5d)$ transition are observed at 433 (SrS:Ce^{3+}) and 430 nm (SrSe:Ce^{3+}), and plateaus due to the fundamental absorption of the host crystals in higher energy region. The vibrational structures on the emission and excitation bands are analyzed by the use of energy matrices in order to determine the coupling constant of spin-orbit interaction ζ_f and the crystal field parameters $V_4^{(f)}$, $V_6^{(f)}$ for the 4f orbit.

Alkaline earth chalcogenides are known as excellent host crystals of phosphors. In particular, the SrS:Ce^{3+} phosphor has been investigated in relation to its availability for cathodo- (1) and electroluminescence devices (2). Its photoluminescence (PL) and excitation spectra, however, are not yet analyzed in detail from the standpoint of the energy terms. The 4f orbit of a Ce^{3+} ion incorporated in a crystal is electrically screened by the $5s^25p^6$ electrons, whereas the 5d orbit splits into the e_g and t_{2g} orbits under the strong influence of an O_h crystal field. The $^2F_{7/2}$ and $^2F_{5/2}$ states originating from the 4f configuration in the LS approximation slightly split into respective substates Γ_6, Γ_7, Γ_8, and Γ_7, Γ_8 in the crystal field. The $^2T_{2g}$ state splits into Γ_7 and Γ_8 substates on account of the spin-orbit interaction. One can observe, in general, two emission bands corresponding to the transitions from the lowest excited state $^2T_{2g}$ to the $^2F_{7/2}$ and $^2F_{5/2}$ states (1-5).

We have already investigated MgS, CaS, and CaSe phosphors activated with Ce^{3+} ions (4, 5). In the present paper, SrS:Ce^{3+} and SrSe:Ce^{3+} phosphors are studied and the results are compared with those obtained in previous investigations, in order to elucidate the effect of host ingredients on the luminescence of Ce^{3+} ions.

Experimental

Preparations.—The host material, SrS, was prepared by sulfurating the purified strontium carbonate at 1000°C for 50 min in a stream of H_2S. On the other hand, SrSe was prepared by reducing the purified strontium selenate at 600°C for 70 min in a stream of H_2. The product, SrSe, was reheated at 1080°C for 30 min in N_2 in order to stabilize it chemically. The details are described in a previous paper (6).

We prepared the SrS:Ce^{3+} phosphor by firing the mixture of the strontium sulfide powder and a small amount of CeF_3 (purity, 99.99%) at 1000°C for 50 min in $N_2 + H_2S$. The SrSe:Ce^{3+} phosphor was prepared in the same manner by the firing of the mixture of the strontium selenide power and CeF_3 at 1050°C for 50 min in N_2, together with a small amount of NaF as flux. In the preliminary experiments it was determined that added NaF is useful in improving the luminescent efficiency of the Ce^{3+} centers and does not produce any additional emission and excitation bands in the spectral range where the measurements were made.

X-ray diffraction patterns for the furnished phosphors showed that they are well crystallized in the rock salt type structure (a = 6.02Å for SrS:Ce^{3+} and 6.25Å for SrSe:Ce^{3+}; Na^+) and that there are no detectable traces of carbonate, selenate, or oxide.

Photoluminescence measurements.—The experimental apparatus used to observe the PL and excitation spectra has been described in the previous paper (6). The digitalized data of the PL signals were stored automatically in a floppy disk through a personal computer with a GP-IB interface. The PL and excitation spectra were drawn on an X-Y plotter after the correction for the spectral sensitivity of the spectroscopic system.

Results and Discussion

Photoluminescence.—Figure 1 shows the PL spectra of the SrS:Ce^{3+} and SrSe:Ce^{3+} phosphors at 300 and 80 K. The emission bands I and II correspond to the transi-

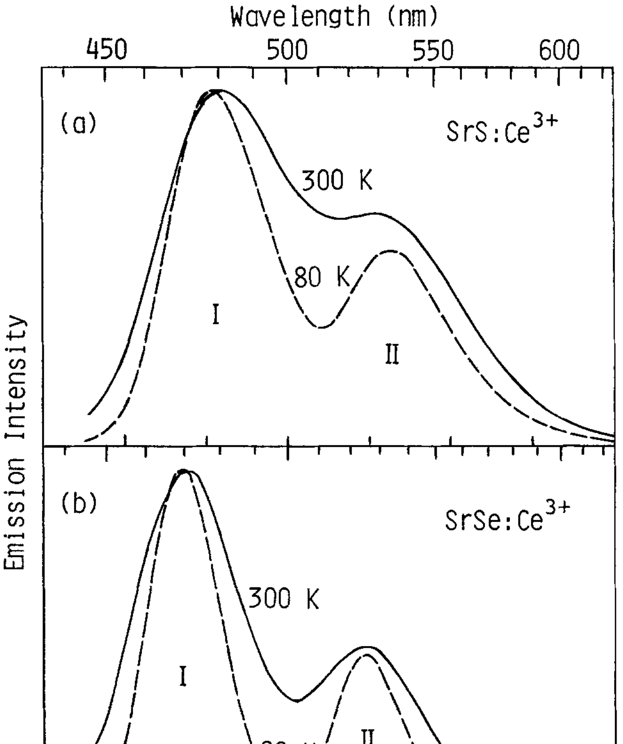

Fig. 1. Photoluminescence spectra of (a) SrS:CeF_3 [0.02 mole percent (m/o)] and (b) SrSe:CeF_3 (0.1 m/o); NaF (1 m/o) at 300 and 80 K, excited at 434 nm.

---

[1] Present address: Sumitomo Electric Industries, Incorporated, Osaka 565, Japan.

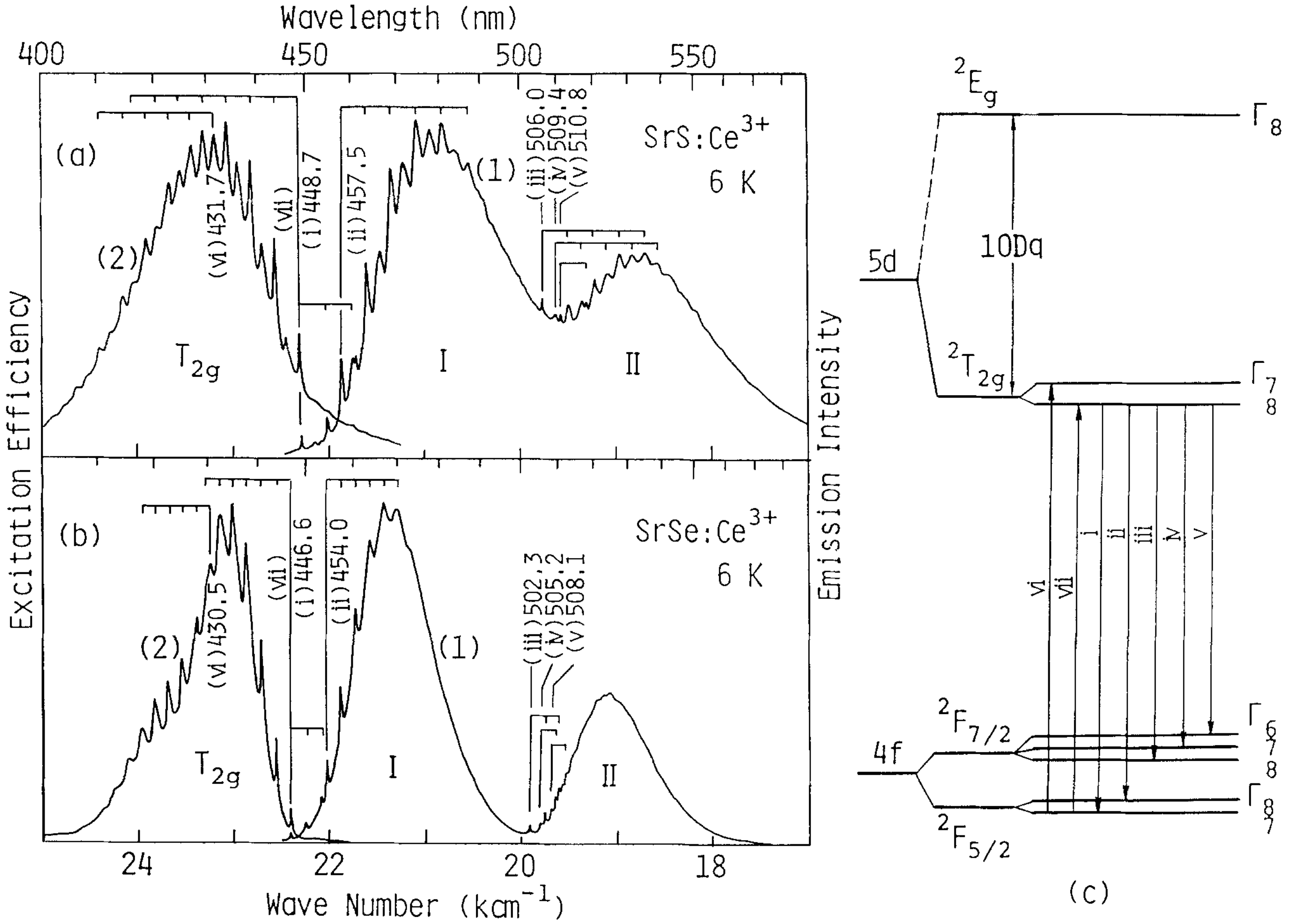

Fig. 2. Vibrational structures of the emission (curve 1) and excitation (curve 2) bands of (a) SrS:CeF$_3$ (0.1 m/o) and (b) SrSe:CeF$_3$ (0.1 m/o); NaF (1 m/o) at 6 K. The emission spectra were obtained under the excitation at 435 nm, and the excitation spectra by observing at 530 nm.(c) Energy levels of a Ce^{3+} ion in an O$_h$ crystal field for the 4f and 5d configurations and electronic transitions (*i-vii*) realized between them at low temperatures.

tions from the $^2T_{2g}$ state to the $^2F_{5/2}$ and $^2F_{7/2}$ states, respectively. The saddle part between the two emission bands becomes markedly deeper at 80 K owing to the suppression of lattice vibrations in the initial state.

Figure 2 shows the vibrational structures of the emission and excitation bands of the SrS:Ce^{3+} and SrSe:Ce^{3+} phosphors at 6 K. The shape of the emission spectra (curve 1) is almost similar to that obtained at 80 K (Fig. 1), except that two phonon series (*i, ii*) appear on the band I and three phonon series (*iii, iv, v*) on the band II. On the excitation band (curve 2) one can also observe well-defined two-phonon series (*vi, vii*). The fact that the zero phonon line of the series (*vii*) on the excitation band just agrees with that of the series (*i*) on the emission band I suggests the excitation band corresponds to the $^2F_{5/2} \to {}^2T_{2g}$ transition. The $^2F_{5/2} \to {}^2E_g$ excitation band cannot be observed, being masked by the fundamental absorption. This makes the higher energy part of the excitation spectra almost similar to the diffused absorption spectra of the corresponding host powder crystal (6). It is cut off, therefore, from the figure.

Table I shows the fequencies, ω_{TO} and ω_{LO}, of the TO and LO phonons of host crystal (7) and the localized phonon frequencies, ω_{ex} and ω_{em}, that is, the intervals of the phonon series observed on the excitation and emission bands, respectively [*cf.* Fig. 2], for some alkaline earth chalcogenide phosphors activated with Ce^{3+} ions. One can see the trends $\omega_{TO} < \omega_{ex} \simeq \omega_{em} < \omega_{LO}$ for the sulfides and $\omega_{TO} \simeq \omega_{ex} \simeq \omega_{em} < \omega_{LO}$ for the selenides. Further research will be needed in order to clarify the mechanism producing these trends.

Energy matrices.—Three energy matrices for the Γ_6, Γ_7, Γ_8 substrates resulting from the 4f configuration and two energy matrices for the Γ_7, Γ_8 substrates resulting from the 5d configuration are shown in the Appendix. The matrix elements of the former and the latter take the form of linear combinations in four energy parameters A_f, ζ_f, $V_4^{(f)}$, $V_6^{(f)}$ and in three ones A_d, ζ_d, 10 Dq, respectively. The notations A_f and A_d mean the energies of the 4f and 5d orbits, respectively, while ζ_f and ζ_d denote the coupling constants of the spin-orbit interaction for both the orbits. The crystal parameter for the 5d orbit is denoted by 10 Dq, whereas those of the fourth and sixth orders for the 4f orbit by $V_4^{(f)}$ and $V_6^{(f)}$, respectively. As these matrices have a rank not higher than two, the secular equations referring to them can be solved algebraically. Owing to the smallness of their nondiagonal elements, each one of their diagonal elements may be considered as expressing approximately the energy of the corresponding state.

Analysis of spectra.—We determined the values of the energy parameters by same procedure as described in the previous papers (4, 5). At this time we only give an

Table I. Frequencies (cm^{-1}) of TO and LO phonons and localized phonons

	ω_{TO}	ω_{LO}	ω_{ex}	ω_{em}
CaS:Ce^{3+}	229	342	278, 282	(a) 294, 293 (b) 294, 294, 294
SrS:Ce^{3+}	185	282	246, 250	(a) 268, 266 (b) 267, 268, 266
CaSe:Ce^{3+}	168	220	168, 166	(a) 168, 167 (b) 169, 168, 168
SrSe:Ce^{3+}	141	201	144, 146	(a) 156, 154 (b) 155, 153, 153
References	(7)	(7)	(5) and this work	

The frequencies (a) and (b) correspond to the phonon series on the emission bands I and II, respectively.

Table II. Comparison of values (cm^{-1}) of energy parameters

	ζ_f	$V_4^{(f)}$	$V_6^{(f)}$	ζ_d	References
MgS:Ce^{3+}	666.5	2957	638.4	644	(4)
CaS:Ce^{3+}	658.3	2711	486	619	(5)
SrS:Ce^{3+}	646.6	2589	339.7	588	This work
CaSe:Ce^{3+}	650.3	2383	317.3	601	(5)
SrSe:Ce^{3+}	652.5	2279	323.7	558	This work

outline of the procedure. Referring to the diagonal elements of the two 5d-matrices [A-4], [A-5] and taking into account the inequality

$$10Dq >> \zeta_d > 0 \qquad [1]$$

one can confirm that $E[\Gamma_7(^2T_{2g})] > E[\Gamma_8(^2T_{2g})]$, where the notation $E[\ \ ]$ means the energy of the state indicated in the brackets. Accordingly the initial state of the five phonon series (*i*) to (*v*) in Fig. 2 is assigned to the $\Gamma_8(^2T_{2q})$ state, and the final states of the phonon series (*vi*) and (*vii*) are assigned as shown in Fig. 2c. For the 5d orbit, the inequality [1] and the secular equations referring to the 5d-matrices [A-4], [A-5] lead to the approximate expression

$$E[\Gamma_7(^2T_{2g})] - E[\Gamma_8(^2T_{2g})] \simeq \frac{3}{2}\zeta_d > 0 \qquad [2]$$

which gives immediately the value of ζ_d. On the other hand, referring to the diagonal elements of the three 4f-matrices [A-1]-[A-3] and taking into account the inequality

$$V_4^{(f)} >> V_6^{(f)} > 0 \qquad [3]$$

which is valid for the octahedral coordination, we can confirm that $E[\Gamma_6(^2F_{7/2})] > E[\Gamma_7(^2F_{7/2})]$, $E[\Gamma_8(^2F_{7/2})]$ and that $E[\Gamma_8(^2F_{5/2})] > E[\Gamma_7(^2F_{5/2})]$. This permits us to conclude that the final state of the phonon series (*v*) can be identified with the $\Gamma_6(^2F_{7/2})$ state and that those of the phonon series (*i*) and (*ii*) with the $\Gamma_7(^2F_{5/2})$ and $\Gamma_8(^2F_{5/2})$ states, respectively. The assignment of the two pnonon series (*iii*) and (*iv*) to the two transitions $\Gamma_8(^2T_{2g}) \rightarrow \Gamma_7$, $\Gamma_8(^2F_{7/2})$ produces two possibilities, one of which is to be alternatively adopted. The values of the energy parameters for the 4f orbit are determined by the method of least squares so that the positions of the zero phonon lines and the corresponding roots of the secular equations may coincide with each other as well as possible. The inequality [3] and the restriction that ζ_f should be nearly equal to that of a free Ce^{3+} ion [$\simeq$ 643.7 cm^{-1} (8)] lead to a unique assignment as shown in Fig. 2c (4, 5).

The values of the energy parameters calculated are shown in Table II together with those of other alkaline earth chalcogenide phosphors activated with Ce^{3+} ions. The value of the parameter ζ_f remains nearly unchanged for various host crystals owing to the electric screening, whereas the values of ζ_d, $V_4^{(f)}$, and $V_6^{(f)}$ decrease gradually as the ionic radius of host ingredients increases. It has also been found that the parameter ζ_f for other trivalent rare earth ions is conspicuously independent of host ingredients (9).

Manuscript submitted Jan. 26, 1987; revised manuscript received June 5, 1987.

Okayama University assisted in meeting the publication costs of this article.

APPENDIX

Energy Matrices

1. Energy matrices for the 4f configuration in an O_h symmetry (4, 5)

$$E[\Gamma_6(^2F_{7/2})] = A_f + \frac{3}{2}\zeta_f + \frac{2}{99}V_4^{(f)} + \frac{400}{1287}V_6^{(f)} \qquad [A\text{-}1]$$

$$\begin{array}{c|cc}
 & \Gamma_7(^2F_{7/2}) & \Gamma_7(^2F_{5/2}) \\
\hline
\Gamma_7(^2F_{7/2}) & A_f + \frac{3}{2}\zeta_f - \frac{2}{77}V_4^{(f)} + \frac{80}{429}V_6^{(f)} & \frac{4\sqrt{5}}{77}V_4^{(f)} + \frac{20\sqrt{5}}{143}V_6^{(f)} \\
\Gamma_7(^2F_{5/2}) & & A_f - 2\zeta_f - \frac{2}{21}V_4^{(f)}
\end{array} \qquad [A\text{-}2]$$

$$\begin{array}{c|cc}
 & \Gamma_8(^2F_{7/2}) & \Gamma_8(^2F_{5/2}) \\
\hline
\Gamma_8(^2F_{7/2}) & A_f + \frac{3}{2}\zeta_f + \frac{2}{693}V_4^{(f)} - \frac{320}{1287}V_6^{(f)} & \frac{-4\sqrt{3}}{77}V_4^{(f)} + \frac{50\sqrt{3}}{429}V_6^{(f)} \\
\Gamma_8(^2F_{5/2}) & & A_f - 2\zeta_f + \frac{1}{21}V_4^{(f)}
\end{array} \qquad [A\text{-}3]$$

2. Energy matrices for the 5d configuration in an O_h symmetry (4, 5)

$$E[\Gamma_7(^2T_{2g})] = A_d - 4Dq + \zeta_d \qquad [A\text{-}4]$$

$$\begin{array}{c|cc}
 & \Gamma_8(^2E_g) & \Gamma_8(^2T_{2g}) \\
\hline
\Gamma_8(^2E_g) & A_d + 6Dq & \sqrt{\frac{3}{2}}\zeta_d \\
\Gamma_8(^2T_{2g}) & & A_d - 4Dq - \frac{1}{2}\zeta_d
\end{array} \qquad [A\text{-}5]$$

REFERENCES

1. For example, F. Okamoto and K. Kato, *This Journal*, **130**, 432 (1983).
2. For example, S. Tanaka, Y. Mikami, H. Deguchi, and H. Kobayashi, *Jpn. J. Appl. Phys.*, **25**, L225 (1986).
3. S. P. Keller and G. D. Pettit, *J. Chem. Phys.*, **30**, 434 (1959).
4. S. Asano, N. Yamashita, and T. Ohnishi, *Phys. Status Solidi B*, **99**, 661 (1980).
5. S. Asano, N. Yamashita, and Y. Ogawa, *ibid.*, **118**, 89 (1983).
6. N. Yamashita, T. Ohira, H. Mizuochi, and S. Asano, *J. Phys. Soc. Jpn.*, **53**, 419 (1984).
7. K. Kaneko, K. Morimoto, and T. Koda, *ibid.*, **51**, 2247 (1982).
8. B. G. Wybourne, "Spectroscopic Properties of Rare Earths," p. 41, John Wiley & Sons, Inc., New York (1965).
9. W. T. Carnall, P. R. Fields, and K. Rajnak, *J. Chem. Phys.*, **49**, 4429 (1968).